The phase diagram of hard spheres in a periodic external potential

LETTER TO THE EDITOR

The phase diagram of hard spheres in a periodic external potential

J L Barrat† and H Xu‡

† Laboratoire de Physique, Ecole Normale Supérieure de Lyon, 46 Allée d'Italie, 69364 Lyon Cédex 07, France
‡ University Chemical Laboratory, Lensfield Road, Cambridge CB2 1EW, UK

Abstract. The density-functional theory has been applied to calculating the phase diagrams of a hard-sphere system in a one-dimensional periodic external potential. The results show that when the wavelength of the external potential is comparable to the hard-sphere solid lattice spacing, the freezing transition occurs at sensitively lower densities. The possibility of a smectic-B-like phase has been investigated in the case of large wavelengths. Two versions of the density-functional theory, the modified weighted-density approximation and generalized effective liquid approximation are shown to give similar phase diagrams.

The freezing transition induced by a periodic external potential has already been observed in experiments [1], where strongly interacting colloidal particles confined between two plates are observed to form a two-dimensional triangular lattice when crossed laser beams produce a one-dimensional modulation of the spatial density in the fluid. In the present work we investigate the phase transitions of a HS fluid when a one-dimensional periodic external potential is applied to it. Compared to an earlier similar study [2] where a three-dimensional modulation has been applied to the HS fluid, the present form of external potential is closer to a simple and real experimental situation. As a standard tool for studying the freezing transition, the density-functional theory (DFT) [3] will be used in our study. We have carried out calculations separately with the modified weighted-density approximation (MWDA) [4] and generalized effective liquid approximation (GELA) [3]. Since both theories are very successful in predicting the freezing of unconstrained HS systems, we intend to compare their predictions when an external potential is applied.

We first recall the formalism of DFT for classical non-uniform systems. The free energy is a functional of the one-particle density $\rho(\boldsymbol{r})$

$$F[\rho] = F_{\text{id}}[\rho] + F_{\text{ex}}[\rho] + \int \mathrm{d}\boldsymbol{r}\, \rho(\boldsymbol{r}) V_{\text{ext}}(\boldsymbol{r}) \tag{1}$$

where F_{id} is the free energy of an ideal-gas system

$$\beta F_{\text{id}} = \int \mathrm{d}\boldsymbol{r}\, \rho(\boldsymbol{r})\bigl(\ln(\rho(\boldsymbol{r})\Lambda^3) - 1\bigr) \tag{2}$$

with Λ the thermal wavelength. $V_{\text{ext}}(\boldsymbol{r})$ is the external potential which in the present study is assumed to be of the form

$$V_{\text{ext}}(\boldsymbol{r}) \equiv V_{\text{ext}}(z) = -\beta^{-1} U_0 \cos(k_0 z) \tag{3}$$

where U_0 measures the amplitude of the potential and $(0, 0, k_0)$ is the wavevector. F_{ex} is the excess part of the free energy due to interactions between particles. Its second derivative with respect to the density $\rho(\boldsymbol{r})$ is related to the direct correlation function $c(\boldsymbol{r}, \boldsymbol{r}'; [\rho])$

$$\beta \frac{\delta^2 F_{\text{ex}}[\rho]}{\delta\rho(\boldsymbol{r})\delta\rho(\boldsymbol{r}')} = -c(\boldsymbol{r}, \boldsymbol{r}'; [\rho]). \tag{4}$$

The right-hand side of (4) is only reasonably well known for some simple uniform liquids. For the uniform HS fluid, the Percus–Yevick solution $c_{\text{PY}}(|\boldsymbol{r} - \boldsymbol{r}'|, \rho)$ [5] is widely used. We shall also be using it in the present work. For a non-uniform system, one has to relate $F_{\text{ex}}[\rho]$ to that of an uniform system. One assumes in both MWDA and GELA that

$$\phi_{\text{ex}}[\rho] = \phi_{\text{ex}}(\hat{\rho}) \tag{5}$$

where $\phi_{\text{ex}}[\rho] = F_{\text{ex}}[\rho]/N$ is the excess free energy per particle. The condition expressed by (5) can be called a 'thermodynamic mapping' [3]. The density $\hat{\rho}$ of the uniform effective liquid is related to the real density $\rho(\boldsymbol{r})$ via a weighting function $w(\boldsymbol{r}, \boldsymbol{r}', [\rho])$

$$\hat{\rho} = \frac{1}{\rho V} \int \mathrm{d}\boldsymbol{r} \int \mathrm{d}\boldsymbol{r}'\, \rho(\boldsymbol{r})\rho(\boldsymbol{r}') w(\boldsymbol{r}, \boldsymbol{r}', [\rho]). \tag{6}$$

In MWDA, if it is assumed that $w(\boldsymbol{r}, \boldsymbol{r}', [\rho]) = w(|\boldsymbol{r} - \boldsymbol{r}'|, \hat{\rho})$ and one requires $\int \mathrm{d}\boldsymbol{r}\, w(|\boldsymbol{r} - \boldsymbol{r}'|, \hat{\rho}) = 1$, then the weighting function w is determined by the condition

$$\beta \frac{\delta^2 F_{\text{ex}}^{\text{MWDA}}[\rho]}{\delta\rho(\boldsymbol{r})\delta\rho(\boldsymbol{r}')}\Bigg|_{\rho(\boldsymbol{r}) \to \rho_0} = -c(|\boldsymbol{r} - \boldsymbol{r}'|, \rho_0) \tag{7a}$$

where $F_{\text{ex}}^{\text{MWDA}}[\rho] = \int \mathrm{d}\boldsymbol{r}\, \rho(\boldsymbol{r})\phi_{\text{ex}}(\hat{\rho}[\rho])$ according to (5). From (7a) one obtains for $w^{\text{MWDA}}(r, \rho_0)$

$$w^{\text{MWDA}}(r, \rho_0) = -\big(c(r, \rho_0) + \rho_0 \beta \phi_{\text{ex}}''(\rho_0)/V\big)\big/\big(2\beta\phi_{\text{ex}}'(\rho_0)\big). \tag{7b}$$

In GELA, the starting point is the integral form of (4)

$$\beta F_{\text{ex}}[\rho] = -\int \mathrm{d}\boldsymbol{r} \int \mathrm{d}\boldsymbol{r}'\, \rho(\boldsymbol{r})\rho(\boldsymbol{r}') \int_0^1 \mathrm{d}\lambda \int_0^\lambda \mathrm{d}\lambda'\, c(\boldsymbol{r}, \boldsymbol{r}'; [\rho_{\lambda'}]). \tag{8}$$

The effective liquid with $\hat{\rho}$ satisfies a 'structural mapping' besides the 'thermodynamic mapping' (equation (5)). One assumes

$$c(\boldsymbol{r}, \boldsymbol{r}'; [\rho_\lambda]) = c(|\boldsymbol{r} - \boldsymbol{r}'|; \hat{\rho}([\rho_\lambda])) \tag{9}$$

in (8). The functional $\hat{\rho}[\rho]$ is obtained by self-consistently solving the equation

$$\beta\frac{\partial^2\left(\lambda\phi_{\mathrm{ex}}(\hat{\rho}[\lambda\rho])\right)}{\partial\lambda^2} = -\frac{1}{\rho V}\int\mathrm{d}r\int\mathrm{d}r'\,\rho(r)\rho(r')c(|r - r'|, \hat{\rho}[\lambda\rho]) \qquad (10)$$

assuming the functional form

$$\hat{\rho}[\lambda\rho] = \lambda\sum_{n=0}^{\infty}(\lambda - 1)^n a_n[\rho]. \qquad (11)$$

Notice that (10) is readily derived from the expression for $F_{\mathrm{ex}}[\lambda\rho]$ by using equations (8) and (4). For practical reasons it is necessary to truncate (11). As one only needs to know $\hat{\rho}[\rho] \equiv a_0$ in order to calculate $F_{\mathrm{ex}}[\rho]$ according to (5), the convergence of a_0 is a good criterion for this truncation.

The weighting function $w^{\mathrm{GELA}}(|r - r'|; [\rho])$ is easily derived from (5) and (9)

$$w^{\mathrm{GELA}}(|r - r'|; [\rho]) = \left(-\hat{\rho}\int_0^1\mathrm{d}\lambda\int_0^\lambda\mathrm{d}\lambda'\,c(|r - r'|, \hat{\rho}[\lambda'\rho])\right)\left(\beta\phi_{\mathrm{ex}}(\hat{\rho})\right)^{-1}. \qquad (12)$$

We notice that both MWDA and GELA satisfy (4) at the limit $\rho(r) \rightarrow \rho_{\mathrm{l}}$ while in GELA (5) is realized by a 'structural mapping' (equation (9)). From a practical point of view, MWDA is simpler to implement. The connection between the two approximations is discussed in [3].

The determination of the phase diagram proceeds in the usual manner: one first decides, on physical grounds, which phases should be investigated. Each phase is described by a suitably parametrized density $\rho(r)$. The free energy of each phase is then determined at fixed average density, temperature and external potential by minimizing the functional $F[\rho]$ with respect to the parameters of $\rho(r)$. Finally, at a given wavelength of $V_{\mathrm{ext}}(z)$, the phase diagram in the plane (ρ, U_0) is deduced from a double tangent construction on the free energy versus density curves for the various phases. We shall now describe the different phases which have been considered in this work, and the corresponding parametrizations.

Under the external potential, the isotropic fluid becomes modulated along the z direction. Its density is analogous to that of a smectic liquid crystal phase. We denote it as the M_A phase. The modulated density can be expressed by assuming the simple form

$$\rho_{\mathrm{l}}(r) = A\rho_{\mathrm{l}}\exp\left(-s_{\mathrm{a}}\cos(k_0 z)\right) \qquad (13a)$$

where the normalization constant A is such that $(1/V)\int\mathrm{d}r\,\rho_{\mathrm{l}}(r) = \rho_{\mathrm{l}}$, i.e.,

$$A = \left(\frac{1}{\lambda_0}\int_0^{\lambda_0}\mathrm{d}z\,\exp\left(-s\cos(k_0 z)\right)\right)^{-1} = \frac{1}{I_0(s)} \qquad (13b)$$

where $\lambda_0 \equiv 2\pi/k_0$ is the wavelength of $V_{\mathrm{ext}}(z)$ and $I_0(s)$ is the modified Bessel function of zeroth order. The parameter for the minimization of $F^{(l)}[\rho_{\mathrm{l}}]$ at constant average ρ_{l} is the coefficient s_{a}.

Notice that (13a) allows one to recover the linear response when U_0 is small, in which case $s_{\mathrm{a}}(\text{linear response}) = U_0 S(k_0)$ where $S(k)$ is the static structure factor of
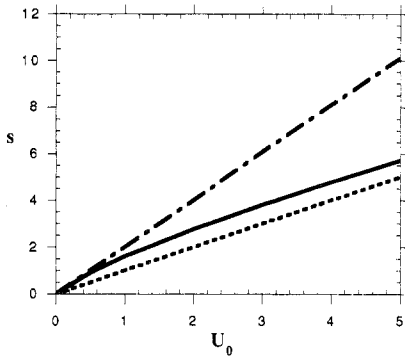
Figure 1. The parameter $s_a(U_0)$ (full curve) in (13a) resulting from the free-energy minimization for the case $k_0\sigma = 6.98$ and $\rho_1 = 0.80$ for which $S(k_0) = 2.03$. In the same plot we have also drawn the curves $s_a(\text{linear response})(U_0)$ (chain curve) and $s_a([2])(U_0) = U_0$ (dotted curve).

the uniform liquid. In figure 1, we compare $s_a(U_0)$ with $s_a(\text{linear response})(U_0)$ and the simple barometric approximation used by the authors of [2], i.e. $s_a([2])(U_0) = U_0$. The comparison is carried out for the case $k_0 = 6.98/\sigma$ where σ is the diameter of the hard spheres. We can see that for this wavelength $s_a(U_0)$ and $s_a([2])(U_0) = U_0$ are reasonably close to each other whereas the linear response is only valid for very small U_0.

The homogeneous HS fluid undergoes a freezing transition towards a close-packed (FCC or HCP) crystalline structure when the pressure or density is increased [6]. With $V_{\text{ext}}(z)$ present, the solid phase is also expected to be a non-ideal hexagonal close-packed crystal with the distance between the compact lattice planes $c = 2\lambda_0$ if the wavelength λ_0 has a value close to the HS lattice spacing. We have assumed the density of the solid phase $\rho_s(r)$ to be a sum of Gaussians centred at the lattice sites

$$\rho_s(r) = \sum_{\{r_i\}} \left(\frac{\alpha_s}{\pi}\right)^{3/2} \exp\left(-\alpha_s(r - r_i)^2\right). \tag{14}$$

The parameter for the free energy minimization is now the width parameter α_s of the Gaussians.

When the wavelength λ_0 is sensibly larger than normal HS lattice spacing, e.g. $\lambda_0 \approx 2d$ where d is the nearest distance between lattice sites, the external potential $V_{\text{ext}}(z)$ is expected to force the modulated fluid to form a new phase with particles being more-or-less locked in the planes of minimum $V_{\text{ext}}(z)$ and forming a close-packed triangular lattice there. The planes are not correlated. In other words, they can slide freely with respect to each other. The density of this phase is analogous to that of a smectic-B liquid-crystal phase. This phase will be denoted M_B, and its density represented as

$$\rho_B(r) = \sum_{l=0}^{\infty} \rho_1(z - z_l)\,\rho_2(R - R_l) \tag{15}$$

where $z_l = l\lambda_0$, $R = (x, y)$; $R_l = lR$ and

$$\rho_1(z) = \begin{cases} (1/\lambda_0)A\exp(-s_B\cos(k_0z)) & \text{if } 0 \le z \le \lambda_0 \\ 0 & \text{elsewhere} \end{cases} \tag{16}$$

and

$$\rho_2(\boldsymbol{R}) = \sum_{\{\boldsymbol{R}_s\}} \left(\frac{\alpha_B}{\pi}\right) \exp(-\alpha_B(\boldsymbol{R} - \boldsymbol{R}_s)^2) \tag{17}$$

where $\{\boldsymbol{R}_s\}$ are the vectors of a two-dimensional triangular lattice and A is a function of s_B defined as in (13b). The free energy must now be minimized with respect to the parameters s_B and α_B. In calculating the free energy for this phase, a difficulty arises from the fact that the two-dimensional crystals in the different planes are supposed to be uncorrelated. We incorporate this constraint in the calculation of the free energy by averaging over all of the possible orientations and origins for the triangular lattices when calculating integrals such as (6).
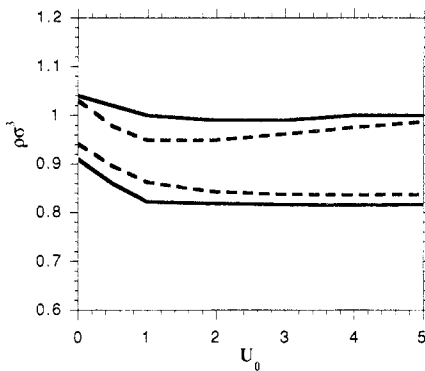
Figure 2. The phase diagram for wavevector $k_0\sigma = 6.98$. The liquid and solid coexistence densities $\rho_l\sigma^3$ (lower curves) and $\rho_s\sigma^3$ (upper curves) are drawn versus the strength of the external potential U_0. The full curves are results from MWDA and the broken curves are those from GELA.

We have computed the phase diagram for the three different phases described above for two wavelengths of the external potential. In the first case, $k_0\sigma \equiv q_0 = 6.98$. This value of q_0 corresponds to the maximum of $S(k)$ of homogeneous HS fluid at freezing density ($\rho\sigma^3 = 0.943$). This is a case where $\lambda_0 \approx d$. Hence the freezing transition M_A–non-ideal HCP will be favoured by $V_{ext}(z)$ and the phase M_B is unlikely the appear. The corresponding phase diagram $\{\rho_l(U_0), \rho_s(U_0)\}$ is shown in figure 2 where we notice that because of the presence of $V_{ext}(z)$, freezing does indeed occur at a lower density ρ_l. The solid density ρ_s is also lowered. But the gap between the liquid and solid densities remains finite. Figure 2 also shows that the MWDA and the GELA give very similar phase diagrams. The other situation we investigated is the case $q_0 = 3$ or $\lambda_0/\sigma = 2.1$. The planes of minimum $V_{ext}(z)$ are much further apart than spacing of close-packed planes in a HS crystal. We would then expect to observe the 'M_B' phase when U_0 is strong enough. Nevertheless, we have found that neither MWDA nor GELA could predict a stable M_B phase for U_0 up to 10. The reason might be that the curvature of our $V_{ext}(z)$ is not strong enough to confine particles into planes. Another result worth noticing in this case is that an effective uniform fluid for the phase M_A can no longer be found when U_0 is too large ($U_0 > 10$ for MWDA and a little larger for GELA). It is possible that (13a) is not a good approximation for such large values of U_0. The result may also indicate the existence of other more complicated phases promoted by

the external potential. At this stage some experimental evidence is needed to give a hint at their symmetry. In the case of $q_0 = 3$, the freezing transition is not favoured by $V_{ext}(z)$. At coexistence, $\rho_l(U_0 \neq 0)$ is slightly smaller than the unconstrained value $\rho_l(U_0 = 0)$ and $\rho_s(U_0 \neq 0)$ is slightly larger than $\rho_s(U_0 = 0)$.

We have shown with this simple study that a periodic external potential with suitable wavelength favours the freezing transition. This result agrees with previous studies [1, 2]. The situation we presented can be realized in experiments. We have also characterized one of the more complex phases that may form because of the external potential. The smectic-B-like phase we investigated does not seem to be stable within our approximations for the form of potential we have used. We still expect these complex phases to occur in real systems even with a simple external potential. Further studies, both theoretical and experimental, are needed to describe them better. Finally, we have shown that MWDA and GELA give similar phase diagrams for hard spheres in an external potential.

References

[1]   Chowdhury A, Ackerson B J and Clark N A 1985 *Phys. Rev. Lett.* **55** 833
[2]   Xu H and Baus M 1986 *Phys. Lett.* **11A** 127
[3]   Lutsko J F and Baus M 1990 *Phys. Rev. A* **41** 6647
[4]   Denton A R and Ashcroft N W 1989 *Phys. Rev. A* **39** 4701
[5]   Hansen J-P and McDonald I R 1986 *Theory of Simple Liquids* 2nd edn (London: Academic)
[6]   Alder B J and Wainwright T E 1962 *Phys. Rev.* **127** 359